Wintertime Air Quality in Lumbini, Nepal: Sources of Fine Particle Organic Carbon

Md. Robiul Islam, Tianyi Li, Khadak Mahata, Nita Khanal, Benjamin Werden, Michael Giordano, Puppala Siva Praveen, Narayan Babu Dhital, Anobha Gurung, Arnico K. Panday, et al.

ACS EARTH AND SPACE CHEMISTRY

http://pubs.acs.org/journal/aesccq

Article

Wintertime Air Quality in Lumbini, Nepal: Sources of Fine Particle Organic Carbon

Md. Robiul Islam, Tianyi Li, Khadak Mahata, Nita Khanal, Benjamin Werden, Michael R. Giordano, P. S. Praveen, Narayan Babu Dhital, Anobha Gurung, Arnico K. Panday, Indu Bikram Joshi, Shankar Prasad Poudel, Yanbo Wang, Eri Saikawa, Robert J. Yokelson, Peter F. DeCarlo, and Elizabeth A. Stone*

Cite This: *ACS Earth Space Chem.* 2021, 5, 226–238

Read Online

ACCESS | Metrics & More | Article Recommendations | Supporting Information

ABSTRACT: The Indo-Gangetic Plains (IGP) experience high levels of airborne particulate matter (PM), especially during the dry season. Contributing to PM are natural and anthropogenic emissions and the atmospheric transformation of gases to form particles. Regional smog events occur frequently during wintertime and provide an atmospheric medium for aerosol processing. Here, we investigate the chemical composition and sources of PM at a representative site in the northern IGP during the second Nepal Ambient Monitoring and Source Testing Experiment (NAMaSTE 2). In Lumbini, Nepal, the 24 h average $PM_{2.5}$ and PM_{10} concentrations ranged 48–295 and 60–343 $\mu g\ m^{-3}$, respectively, from December 20, 2017, to January 1, 2018. On average (± standard deviation), $PM_{2.5}$ was composed of 39 ± 7% organic carbon (OC), 5 ± 2% elemental carbon (EC), and 20 ± 6% secondary inorganic ions (ammonium, nitrate, and sulfate), 2.0% chloride, and 1.3% potassium. Biomass burning was a major PM source, indicated by a median levoglucosan concentration of 3.5 $\mu g\ m^{-3}$. Secondary organic aerosol (SOA) derived from biomass burning was indicated by high concentrations of nitromonoaromatic compounds (e.g., 4-nitrocatechol peaking at 435 ng m^{-3}). During periods of fog, characterized by high relative humidity (RH) and relatively low solar radiation, nitroaromatic concentrations dropped despite levoglucosan remaining high, indicating that their formation was suppressed. Chemical signatures of SOA indicated that volatile organic compound (VOC) precursors were primarily combustion-derived, with small contributions from biogenic VOC. Through molecular markers and chemical mass balance (CMB) modeling, sources of $PM_{2.5}$ OC were identified as cow dung burning (24 ± 16%), other biomass burning (20 ± 7%), plastic/garbage burning (4.7 ± 3.2%), vehicle emissions (3.1 ± 1.4%), coal combustion (0.3 ± 0.2%), and SOA from monoaromatic VOC (4.1 ± 0.8%), diaromatic VOC (8.9 ± 4.0%), cresol (0.3 ± 0.4%), isoprene (0.4 ± 0.2%), monoterpenes (1.5 ± 0.6%), and sesquiterpenes (3.2 ± 0.7%). Understanding the levels of PM in Lumbini, along with its chemical composition and sources of OC, contributes to a better understanding of regional air quality episodes in the IGP.

KEYWORDS: *atmospheric aerosols, carbonaceous aerosol, source apportionment, chemical mass balance, molecular markers, garbage burning, biomass burning, Indo-Gangetic plains*

INTRODUCTION

The winter season in the Indo-Gangetic Plains (IGP) is characterized by severe haze and high particulate matter (PM) concentrations.[1−4] Frequent exceedance of the PM level over the World Health Organization (WHO) guidelines is well documented.[5−9] Negative consequences of regional pollution events include exacerbations of respiratory and cardiovascular diseases,[10,11] increasing incremental lifetime cancer risk,[12−15] harm to agriculture,[3,16] and reduced visibility.[16] Understanding the natural and anthropogenic sources and processes that contribute to airborne particulate matter (PM) is the focus of this study.

Prior studies in Lumbini and elsewhere in Nepal and the IGP have provided insight into sources of PM during wintertime. The most prevalent source of PM is biomass burning as indicated by measurements of levoglucosan,[9,17,18] PAH,[6] and $PM_{2.5}$ to PM_{10} ratios.[19] Regionally, biomass burning includes residential combustion of firewood and

Received: September 25, 2020
Revised: December 17, 2020
Accepted: December 20, 2020
Published: January 12, 2021

https://dx.doi.org/10.1021/acsearthspacechem.0c00269
ACS Earth Space Chem. 2021, 5, 226–238

dung, crop residue burning, and forest fires.[5,20−23] Biomass is a widely used fuel for household cooking and heating[24−26] and in brick kilns[22,27] in South Asian countries. The importance of secondary aerosol formation is indicated by secondary inorganic ions (SO_4^{2-}, NO_3^-, and NH_4^+).[28,29] In the IGP, sources of NH_3, NO_x, and SO_2 include agricultural fertilizer use, animal husbandry,[30] fossil fuel and biomass combustion,[22,31,32] industrial activities, and coal combustion.[33] The IGP region experiences exceptionally high levels of biomass burning,[9,17] and this source is expected to impact regional secondary organic aerosol (SOA) based on the availability of gas-phase precursors and their SOA forming potential.[34,35] Fossil fuel emissions also contribute to PM, as indicated by 60% of total black carbon (BC) contributed by this source.[5] Plastic and garbage burning are also probable sources, as suggested by prior measurements in the region.[17,36] Resuspended dust from vehicle activity on unpaved roads, construction activity, and wind-blown dust are the major sources of coarse particles ($PM_{10-2.5}$: particles with a diameter of 2.5−10 micron) in Lumbini,[5,19] particularly in the dry season.[8]

As part of the second Nepal Ambient Monitoring and Source Testing Experiment (NAMaSTE 2) campaign, this study has the overarching goal to characterize the chemical composition and the sources of wintertime PM in Lumbini, located on the IGP within Nepal. Enabled by recent methodological advances,[37] we assess in the IGP for the first time SOA derived from biomass burning and from aromatic VOC through measurements of particle-phase organic tracers. In addition, we assess the impact of garbage and plastic burning, a globally under-characterized source,[38] by way of the molecular marker 1,3,5-triphenylbenzene.[39] Through chemical mass balance (CMB) source apportionment modeling supported by regional source characterization,[22,23] we provide new insight into the relative impacts of primary and secondary sources. CMB was selected for source apportionment, because of the availability of regionally specific source profiles collected in NAMaSTE and because this model is readily applied to small sample sizes. Such information supports air quality management efforts by providing benchmark concentrations and quantitative assessments of the sources of PM and other hazardous air pollutants.

METHODS

Site Description, PM Sampling, and Other Data Products. Lumbini is a UNESCO World Heritage Site located in the Terai region of southern Nepal. PM samples were collected within the green protected area surrounding Buddha's birthplace on the rooftop of a three-story hotel building (27.462° N, 83.282° E) at approximately 10 m above ground level. Ambient $PM_{2.5}$ and PM_{10} samples were collected from December 20, 2017, to January 1, 2018, using a medium volume sampler (URG-3000 ABC) on to precleaned 47 mm quartz fiber filters (QFFs; Tissuquartz, Pall Life Sciences, East Hills, New York) and Teflon filters (Teflo Membrane, 2.0 μm pore size, Pall Life Sciences). PM samples were collected twice daily, at times corresponding to daytime (9:00 a.m. to 8:00 p.m.) and nighttime (9:00 p.m. to 8:00 a.m.). The sampled filters were transferred to polystyrene Petri dishes lined with precleaned aluminum foil, capped, sealed with Teflon tape, stored frozen in sealed polyethylene bags, and shipped to the University of Iowa for analysis. The samples were stored frozen at −20 °C upon arrival and were analyzed within 6 months of collection.

Additional measurements were conducted at the Lumbini Air Quality Monitoring Station (27.4897 N, 83.2789 E) located 3 km to the north of the PM sampler. These included $PM_{2.5}$ mass concentrations that were measured with a Grimm Environment Dust Monitor-180 (GRIMM Aerosol Technik, Germany) with the instrument inlet positioned 4 m above ground level; 24 h $PM_{2.5}$ mass concentrations were calculated from hourly averages and were reported only for days with >90% data coverage. Meteorology (temperature, relative humidity [RH], solar radiation, wind speed, and wind direction) were measured with a weather sensor (WS700-UMB, Lufft, Fellbach, Germany). Other measurements included imagery from LANCE FIRMS operated by NASA's Earth Science Data and Information System (ESDIS) (https://earthdata.nasa.gov/firms) to determine the presence of fog in the sampling area. Hourly visibility data were retrieved from the Automated Surface Observing System (ASOS) Network for Kathmandu, Nepal, and Lucknow, India (https://mesonet.agron.iastate.edu/request/download.phtml?network=NP__ASOS) and averaged to the times of filter sample collection.

PM, OC, and EC Measurements. PM mass concentrations were measured gravimetrically by the difference of Teflon filter masses before and after the sample collection in a temperature (22 ± 0.5 °C) and humidity (31 ± 6%) controlled environment where the filters were conditioned for 48 h prior to the measurements. Organic carbon (OC) and elemental carbon (EC) were measured by the thermal-optical method using 1.0 cm^2 filter punches as described by Schauer et al.[40] The uncertainty in OC was propagated from the standard deviation of the field blank (0.13 $\mu g\ cm^{-2}$) and 10% of the measured OC concentration, which is a conservative estimate of the precision error determined by replicate sample analysis. The uncertainty in EC was propagated from the instrumental uncertainty (0.05 $\mu g\ cm^{-2}$), 5% of the measured EC, and 5% of pyrolyzed carbon.

Extraction and Analysis of POA and SOA Tracers. Organic molecular markers were extracted from quartz fiber filters with acetonitrile, extracts were evaporated with a rotary evaporator and mini evaporator (Reacti-Vap I, Thermo Scientific) using a gentle flow of high purity nitrogen gas (PRAXAIR Inc.; Zymark Turbo-Vap II, LV, Caliper Life Science), filtered using a 0.2 μm PTFE filter (Whatman, GE Health Care Life Sciences), and analyzed with gas chromatography coupled to mass spectrometry (GC−MS, Agilent Technologies GC−MS 7890A). Aliquots of these samples were derivatized with a silylation agent *N,O*-bis(trimethylsilyl)-trifluoro-acetamide (Fluka Analytical 99%) to convert active hydrogens (e.g., in hydroxyl and carboxyl functional groups) to trimethylsilyl (TMS) ethers[41] before GC−MS analysis. For the quantification of all organic species, five-point calibration curves of authentic standards or surrogate standards were normalized to isotopically labeled internal standards. Detailed extraction and analysis methods of the filter samples are reported elsewhere,[42] while GC temperature programming and the quantification approaches are described by Stone et al.[21] All organic species concentrations were field blank subtracted. Analytical uncertainties of the measurements were propagated from the standard deviation of the field blanks and 20% of the measured concentration to conservatively account for compound recovery from QFF. For the quantification of levoglucosan, samples were diluted by a factor of 5−6 with a

https://dx.doi.org/10.1021/acsearthspacechem.0c00269
ACS Earth Space Chem. 2021, 5, 226−238

levoglucosan-$^{13}C_6$ internal standard solution, and uncertainties were estimated to increase by 5%.

Analysis of Inorganic Ions. Inorganic ions in $PM_{2.5}$ were extracted into ultrapure water and analyzed by ion-exchange chromatography with conductivity detection (Dionex-ICS 5000) following the method described by Jayarathne et al.[43] with a slight modification to the extraction in which a subfraction of QFF was extracted with 5 mL of ultrapure water by shaking for 10 min (125 rpm) followed by 30 min of sonication (60 sonic per min) and then 10 min additional shaking. The details of the analytical method and detection limit calculations were provided elsewhere.[43] Uncertainties in inorganic ions were propagated from the standard deviation of the field blanks and 10% of the measured concentrations to account for sample recovery from filters, which ranged 93−110%.

CMB Modeling. Source contributions to the $PM_{2.5}$ OC were estimated using the EPA-CMB model (version 8.2) using local and literature source profiles and molecular marker concentrations in ambient $PM_{2.5}$ as model inputs. Source profiles for garbage/plastic waste burning (fire #16), open biomass burning (fire #39), and dung powered traditional cooking stove (fire# 40) were drawn from NAMaSTE in 2015.[23] Other primary and secondary source profiles were drawn from the literature: noncatalyzed gasoline engines,[44] diesel engines,[45] small-scale coal combustion,[46] isoprene, monoterpene, sesquiterpene, and toluene-derived SOA,[47] aromatic SOA from naphthalene and methylnaphthalene,[48] and nitroaromatic SOA from cresol.[37] Contributions from brick kilns in the IGP that are fueled by cofired biomass and coal are expected to be included in the OC apportioned to the source categories of biomass and coal. The CMB model generated negative contributions in seven instances for coal combustion and once for garbage burning; in all the cases, the magnitude of the source contribution was less than or similar to the modeled standard error, indicating that these negative source contributions were not statistically significant. Negative source contributions were considered zero in time series and were excluded from the calculation of averages.

Statistical Analysis. Before performing any statistical analysis, data points with values below detection limits were replaced with the limit of detection (LOD)/$\sqrt{2}$.[49] Performing the Anderson−Darling normality test, concentrations of all the species were found to be either normally or log-normally distributed, thus Pearson's correlation (r) was employed for correlation analysis. Two sample t-tests were used to compare the means of daytime and nighttime concentrations. Correlation analysis was done in SPSS (version 25), all other statistical tests were performed in Minitab (version 17), and significance was assessed at the 95% confidence interval ($p \leq 0.05$).

RESULTS AND DISCUSSION

In the following sections, we discuss $PM_{2.5}$ and PM_{10} mass concentrations, $PM_{2.5}$ composition, and sources of OC. Given the high concentration of $PM_{2.5}$ relative to coarse particles ($PM_{10-2.5}$) we provide detailed compositional information of $PM_{2.5}$, including analysis of water-soluble inorganic ions and organic molecular markers to identify and track sources of OC. Emphasis is placed on major sources and those with emerging importance in the region: fossil fuel combustion, garbage burning, biomass burning, and SOA. Results of the source apportionment of $PM_{2.5}$ OC are subsequently discussed, with a focus on assessing the absolute and relative impact of these primary and secondary sources.

$PM_{2.5}$ and PM_{10} Concentrations, Their Ratios, and Composition (OC, EC, and Inorganic Ions). PM mass and its composition during the winter of 2017−2018 in Lumbini are summarized in Table 1 and Figure 1, and the day−night variations are summarized in Table S1. The 11 h $PM_{2.5}$ and PM_{10} concentrations ranged 48−295 and 60−343 $\mu g\ m^{-3}$, respectively. All daily average measurements exceeded the WHO guidelines of 25 and 50 $\mu g\ m^{-3}$, respectively. The PM concentrations observed in this study period are similar in magnitude to those persisting from November 2017 to March 2018 in Lumbini, which includes the dry winter season (Figure S1). NASA's MODIS/Terra satellite reflectance images (https://earthdata.nasa.gov/firms) showed that there was regional fog throughout the IGP region during the sampling period that exacerbated after December 23, 2017. There was no rain during the sampling period, which is typical in the dry winter season. During this study period, visibility at the Lucknow, India airport located 240 km southeast of Lumbini and averaged over the times of filter sampling ranged 0.14−2.6 km. Compared to Kathmandu, Nepal, the visibility in Lucknow was much lower reflecting the hazier conditions in the IGP (Figure S2).

Table 1. Concentrations ($\mu g\ m^{-3}$) of PM_{10} Mass; $PM_{2.5}$ Mass; and $PM_{2.5}$ Composition, Including OC, EC, and Inorganic Ions in Lumbini from December 20, 2017, to January 1, 2018[a,b]

species	mean ± SD	median	range
PM_{10} mass ($\mu g\ m^{-3}$)	157.8 ± 66.0	155.5	59.5−343
$PM_{2.5}$ mass ($\mu g\ m^{-3}$)	130.1 ± 58.5	124.2	47.5−295
OC ($\mu gC\ m^{-3}$)	55.3 ± 15.8	56.4	28.4−88.3
EC ($\mu gC\ m^{-3}$)	6.5 ± 2.4	5.9	3.7−12.4
inorganic ions ($\mu g\ m^{-3}$)			
ammonium	8.1 ± 4.2	6.9	3.3−21.6
sodium	0.12 ± 0.05	0.11	0.03−0.24
potassium	1.61 ± 0.55	1.61	0.86−3.10
nitrate	11.6 ± 6.7	9.9	3.7−33.0
sulfate	7.7 ± 4.7	6.7	2.4−22.7
chloride	2.7 ± 1.3	2.7	0.78−6.20
fluoride	0.10 ± 0.05	0.10	0.02−0.22

[a]Calcium and magnesium concentrations were above the detection limit in only one sample and are not reported here. [b]SD = Standard deviation.

The ratio of $PM_{2.5}$ to PM_{10} mass averaged 78% indicating the predominance of fine particles relative to $PM_{10-2.5}$. $PM_{2.5}$ was primarily OC 39 ± 7% (Figure 1), with an average OC:EC of 9.0. Secondary inorganic ions, ammonium (NH_4^+), nitrate (NO_3^-), and sulfate (SO_4^{2-}) contributed to a combined 20.4% of $PM_{2.5}$, indicating secondary aerosol formation. Chloride and potassium contributed 2.0% and 1.3% of $PM_{2.5}$, respectively, indicative of biomass burning.[23,50] The corresponding average chloride concentration in Lumbini was 2.7 $\mu g\ m^{-3}$, which is comparable to the concentrations of this species at some of the highly polluted cities in Asia.[36,51,52] The relatively high concentrations of chloride in PM are expected to co-occur with volatile chlorine-containing gases,[36] and are likely to result from dung burning, crop residue burning, and garbage burning (as discussed subsequently). High levels of chloride are expected to contribute to multiphase chlorine chemistry that

https://dx.doi.org/10.1021/acsearthspacechem.0c00269
ACS Earth Space Chem. 2021, 5, 226−238

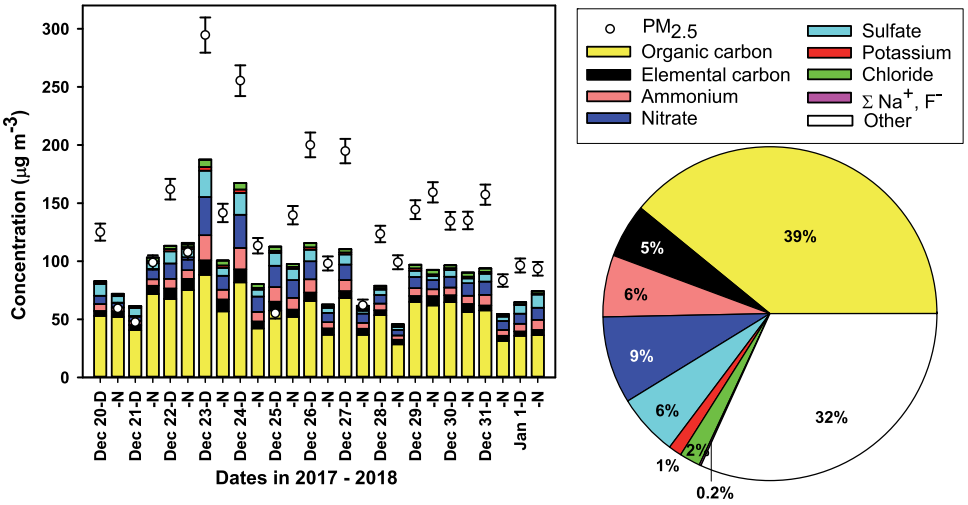

Figure 1. Time series of $PM_{2.5}$ mass loading and its components (organic carbon, elemental carbon, and water-soluble ions) during the sampling period. Calcium and magnesium concentrations were above the detection limit in only one sample and are not reported here.

increases radical production and influences ozone production, especially in polluted environments.[53] Generally, these observations are consistent with previously observed OC:EC and mass contributions for inorganic ions in the IGP.[9,29,54] The measured $PM_{2.5}$ components (Figure 1) accounted for an average of 68% of the measured $PM_{2.5}$ mass. We estimate that approximately 25% or more of $PM_{2.5}$ mass is composed of elements that comprise organic matter other than carbon (i.e., oxygen, nitrogen, and hydrogen) based on an organic carbon to an organic matter conversion factor of 1.7 measured by aerosol mass spectrometry (AMS) in Kathmandu.[36] Airborne dust, which was not directly measured in this study, may also be a minor contributor to $PM_{2.5}$ mass. $PM_{2.5}$ concentrations were significantly higher during daytime ($p = 0.047$); however, this was largely due to the high daytime $PM_{2.5}$ concentrations on December 23 and 24. When these two daytime periods were excluded, there was no significant day and nighttime difference in $PM_{2.5}$ ($p = 0.137$). OC, ammonium, and sulfate, when normalized to $PM_{2.5}$ mass, did not show any significant diel differences.

Biomass Burning Emissions. The impact of biomass burning on ambient $PM_{2.5}$ in Lumbini is indicated by the exceptionally high concentrations of levoglucosan (1824−5614 ng m^{-3}), (Figure 2a), a well-established molecular marker of cellulose pyrolysis that is used to track biomass burning in the atmosphere.[18] The average concentration of levoglucosan (Table 2) in Lumbini during winter of 2017−2018 was approximately 2−3 times higher than that observed in Lumbini during the postmonsoon (2206 ± 1753 ng m^{-3}) and winter of 2013−2014 (1161 ± 1347 ng m^{-3})[9] as well as in the Kathmandu Valley during premonsoon of 2015 (1230 ± 1154 ng m^{-3}).[36] The average levoglucosan concentration observed in this study was also 2−3 times higher than prior studies in the IGP, including Rajim, India, in October−November 2011 (2258 ± 730.3 ng m^{-3});[55] Delhi, India, during winters of 2006−2008 (1978 ± 971 ng m^{-3});[56] Varanasi, India, during winter 2015−2018 (1101 ± 405 ng m^{-3});[57] and Kanpur, India, during the winter of 2015−2016 (averaging 1363 ± 310 ng m^{-3} in daytime and 1853 ± 412 ng m^{-3} at nighttime).[58] The observed levoglucosan concentrations in Lumbini are among the highest reported globally (Table S2).

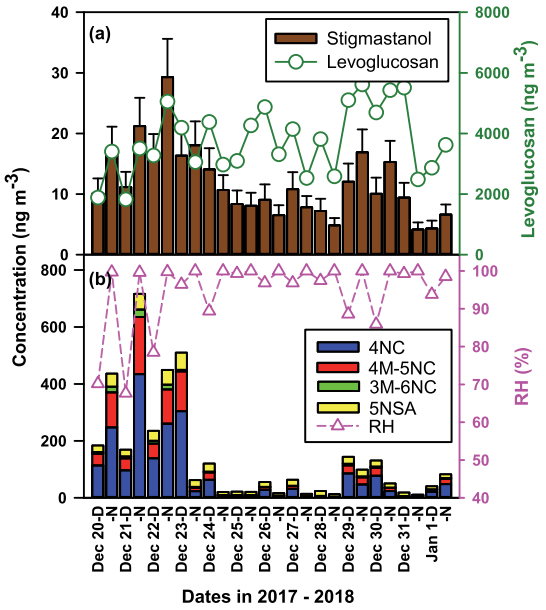

Figure 2. Molecular markers for primary and secondary $PM_{2.5}$ from biomass burning during the winter in Lumbini: (a) stigmastanol [left axis] and levoglucosan [right axis], (b) 4-nitrocatechol (4NC), 4-methyl-5-nitrocatechol (4 M-5NC), 3-methyl-6-nitrocatechol (3 M-6NC), 5-nitrosalicylic acid (5NSA) [left axis] and RH [right axis].

Further insight is gained into the nature of biomass burning, by way of biomass-specific markers. Campesterol is primarily emitted from burning grasses[59] and rice straw and husks[60] and was consistently detected in Lumbini. This finding is consistent with crop residue burning in the IGP and the prevalent south-westerly wind (Figure S3), which usually occurs in the winter months.[6] Stigmastanol, a fecal sterol and molecular marker of dung burning,[60] was detected in all $PM_{2.5}$ samples (Table 2, Figure 2a), consistent with the widespread use of cow dung as fuel in agricultural areas.[61] This is further supported by the observation of coprostanol that is also selective to dung burning.[60] In contrast, retene, a softwood burning tracer,[59,60] was detected only in 77% of the samples with a low concentration (Table 2), suggesting that softwood was a relatively small portion of biomass burning. In comparison to

https://dx.doi.org/10.1021/acsearthspacechem.0c00269
ACS Earth Space Chem. 2021, 5, 226−238

Table 2. Concentrations (ng m^{-3}) of Select Organic Molecular Markers for Primary and Secondary Sources Measured at Lumbini in the Northern IGP[a,b]

species	mean ± SD	median	range
levoglucosan	3747 ± 1106	3563	1824−5614
sterols			
cholesterol	3.9 ± 4.2	2.7	<0.3−16.2
stigmasterol	38.6 ± 31.5	24.7	4.5−120.1
β-sitosterol	70.9 ± 56.1	46.0	9.8−205.6
campesterol	41.3 ± 33.8	25.7	4.2−120.5
coprostanol	1.2 ± 1.5	0.36	0.01−4.7
stigmastanol	11.8 ± 5.8	10.4	4.2−29.3
nitroaromatic compounds (NACs)			
4-nitrocatechol (4NC)	71.7 ± 101.4	30.6	2.1−435
4-methyl-5-nitrocatechol (4 M-5NC)	30.3 ± 47.5	11.7	0.40−201
3-methyl-6-nitrocatechol (3 M-6NC)	4.5 ± 6.7	1.9	0.03−26.3
5-nitrosalicylic acid (5NSA)	21.7 ± 13.2	19.3	8.0−54.9
4-nitrophenol (4NP)	11.3 ± 5.8	10.2	3.5−27.9
2-methyl-4-nitrophenol (2 M-4NP)	12.5 ± 4.2	11.9	5.4−20.7
polycyclic aromatic hydrocarbons (PAHs)			
1,3,5-triphenylbenzene	1.62 ± 0.87	1.27	0.57−4.0
∑ PAHs[c]	54.4 ± 28.1	51.0	18.5−120.8
hopanes			
17α(H)-21β(H)-hopane	0.35 ± 0.11	0.33	0.16−0.55
17β(H)-21α(H)-30-norhopane	0.31 ± 0.11	0.31	0.16−0.55
17α(H)-22,29,30-trisnorhopane	0.16 ± 0.10	0.17	<0.04−0.37
aromatic SOA tracers			
DHOPA	17.8 ± 6.1	16.7	9.9−34.2
phthalic acid	183 ± 91	148.6	11.5−85.8
4-methylphthalic acid	32.2 ± 16.2	29.6	
terephthalic acid	17.4 ± 3.2	16.6	10.4−27.8
isophthalic acid	339 ± 106	314	199−646
isoprene, monoterpene, and sesquiterpene SOA tracers			
2-methylglyceric acid	10.3 ± 3.2	11.3	2.4−15.0
2-methylthreitol[d]	6.3 ± 2.6	7.1	1.1−10.1
2-methylerythritol[d]	11.0 ± 2.9	10.9	3.2−19.0
3-hydroxyglutaric acid[e]	94.7 ± 18.4	92.5	17.1−134
3-acetyladipic acid[e]	82.2 ± 18.4	78.8	41.7−128
β-caryophyllinic acid[e]	40.6 ± 14.7	38.2	20.3−86.1

[a]Day and nighttime concentrations of each species are reported in Table S4, and measurements of individual PAH are summarized in Table S5. [b]SD = standard deviation; BDL = below detection limit. [c]Concentrations of all other individual PAHs are reported in Table S4. [d]Semiquantified using meso-erythritol calibration. [e]Semiquantified using *cis*-pinonic acid calibration.

the Kathmandu Valley and Himalayan foothills, the campesterol to OC ratio was 4−9 times higher and stigmastanol to OC ratio was approximately 2−3 times higher in Lumbini,[20,36] reflecting the larger impact of crop residue and cow dung burning in the IGP.

Biomass Burning Impacts on SOA Formation. The impacts of biomass burning on SOA formation were examined by way of four nitroaromatic compounds (NACs): 4-nitrocatechol (4NC), 4-methyl-5-nitrocatechol (4 M-5NC), 3-methyl-6-nitrocatechol (3 M-6NC), and 5-nitrosalicylic acid (5NSA).[37,62] NACs can form by atmospheric oxidation of phenolic compounds[70−75] that are products of lignin pyrolysis.[59,76] Together, the concentrations of these four NACs ranged 63.2−716 ng m^{-3}, with 4NC being the most abundant (Table 2, Figure 2b). NAC concentrations in Lumbini were the highest observed worldwide to date, except for Rondônia, Brazil during an intense biomass burning period in 2002 (Table S2 and Figure 3). 4-Nitrocatechol, 4-methyl-5-nitrocatechol, 3-methyl-6-nitrocatechol, and 5-nitrosalicylic acid were highly intercorrelated (r = 0.88−0.99; $p < 0.001$; Table S3), consistent with prior studies,[42,69] supporting their formation from a common source in Lumbini.

NACs were significantly higher prior to December 23 (averaging 351 ng m^{-3}) than during the remainder of the study (72.8 ng m^{-3}, p = 0.01), although levoglucosan concentrations (indicative of primary biomass emissions) remained elevated throughout (Figure 2b). Daytime RH was lower prior to December 23, compared to the latter part of the study (Figure 2b, Figure S3) when the regional fog was thicker throughout the IGP region as indicated by NASA's MODIS/Terra satellite reflectance images (https://earthdata.nasa.gov/firms). Additional evidence of dense fog after December 23 is also indicated by lower actinic flux and relatively high daytime RH (Figure S3). The humidity-dependent production of aerosol phase nitrogen-containing organic compounds was previously demonstrated by large decreases in the NO_2^+ signal (by 40%) when humidity increased from 2 to 90% RH.[77] Thus, humidity is expected to suppress the condensation reaction (shown with reversible arrows) that produces NACs (Scheme 1).[70−74,78]

Meanwhile, low to moderate RH (defined as <5 and 30%, respectively) promotes the formation of NACs.[79] An increase in NAC concentrations was observed from the daytime of December 29 through the daytime of December 30, when fog lessened and the daytime RH decreased. While the suppression of NAC formation by RH has been observed in the laboratory, these are the first such observations made in the field. This suggests that the extent of biomass burning-derived SOA depends on atmospheric water content.

Prior studies in the IGP and in the Kathmandu Valley have reported high concentrations of light-absorbing aerosol, particularly in the winter.[7,80−82] In Lumbini, light-absorbing aerosol has been attributed to biomass burning and light absorption differs across foggy, hazy, and sunny days.[81] The NAC concentrations are dramatically reduced on foggy days, indicating that NAC contributes to temporal variability in light-absorbing aerosol response to fog. Following that NACs are major components of brown carbon associated with primary biomass burning emissions and secondary aerosol derived from biomass burning precursors,[83,84] it is expected that NACs contribute substantially to brown carbon in Lumbini and the greater IGP region.

Molecular Markers for Garbage Burning and Fossil Fuel Combustion. 1,3,5-Triphenylbenzene (TPB) is a byproduct of plastic burning.[23,39] TPB has been used to assess plastic and garbage burning in ambient air.[36,85] The average mass concentration of TPB ranged from 0.6 to 4.0 ng m^{-3} and averaged 1.6 ± 0.9 ng m^{-3} (Table 2, Figure 4a). TPB accounted for proportionally more OC during nighttime than daytime, reflecting diurnal variation in this source. The average concentration of TPB in Lumbini is approximately twice that observed in the Kathmandu Valley during April 2015,[36] suggesting a greater influence of this source, which could result from different garbage compositions, a different plastic combustion emissions profile,[39] and/or seasonal influences. TPB was also detected in Chennai, a large tropical city in Southern India at higher concentrations (4.24 ± 3.54 ng m^{-3}) during January−February 2007,[86] consistent with widespread

https://dx.doi.org/10.1021/acsearthspacechem.0c00269
ACS Earth Space Chem. 2021, 5, 226−238

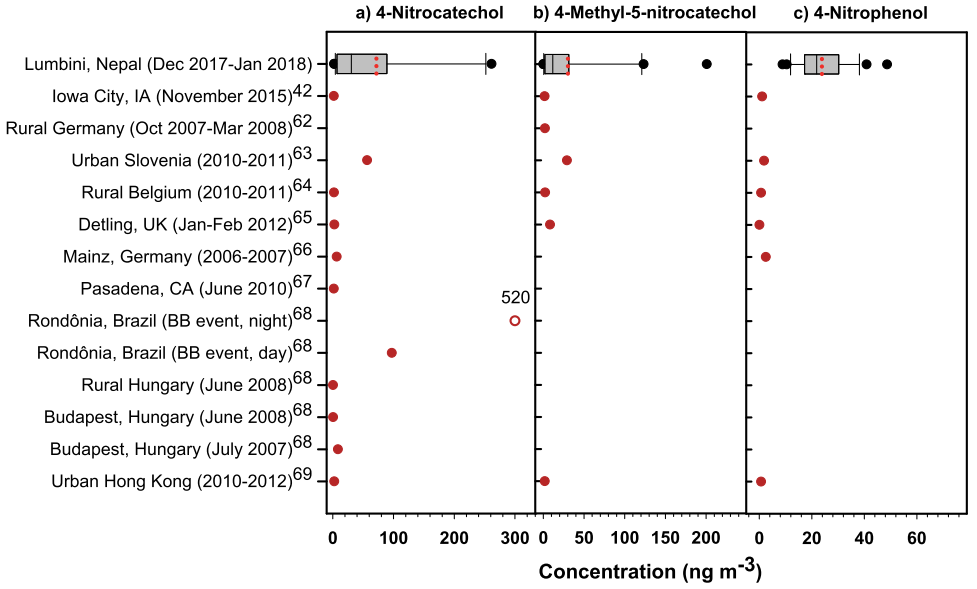

Figure 3. Concentrations of select nitromonoaromatics (NACs) in Lumbini and prior studies. The Lumbini plot shows the 25th and 75th percentiles (box), range (bars), median (black vertical line), mean (red dotted line), and outliers (black dots). Mean concentrations (filled red dots) and one off-scale value (open red circle) are shown for Al-Naiema and Stone,[42] Iinuma et al.,[62] Kitanovski et al.,[63] Kahnt et al.,[64] Mohr et al.,[65] Zhang et al.,[66] Zhang et al.,[67] Claeys et al.,[68] and Chow et al.[69]

Scheme 1. Formation of Nitroaromatic Compounds from Phenolic Compounds adapted from Grosjean et al.[78]

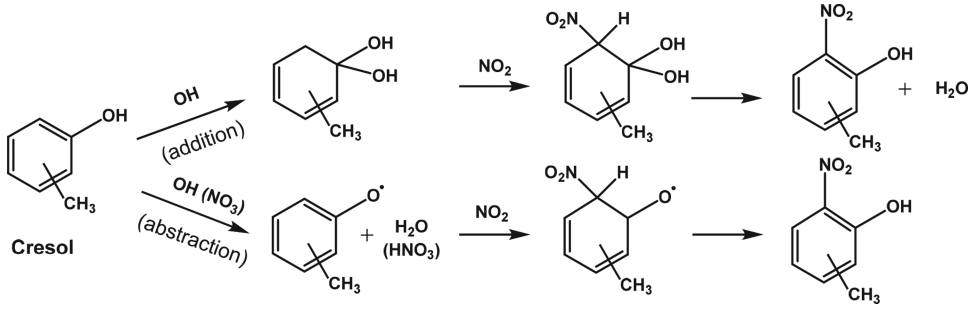

garbage burning in South Asia,[38] particularly during the winter months.

Hopanes are general molecular markers of fossil fuels.[87] Among this class of compounds, 17α(H)-21β(H)-hopane and 17β(H)-21α(H)-30-norhopane were detected in all samples, while 17α(H)-22,29,30-trisnorhopane was detected in 80 percent of samples (Figure 4b). The observed hopane concentrations in Lumbini (Table 2) were much lower (0.46−1.34 ng m^{-3}) than those observed in four mega-cities in India (1.10−22 ng m^{-3}),[88] indicating a lesser influence of fossil fuel combustion. Fossil fuel uses in the IGP include diesel-powered vehicles and groundwater pumps for irrigation,[89,90] gasoline fuel for light vehicles like motorcycles, and coal used to fire brick kilns.[22] The ratio of 17α(H)-21β(H)-hopane, 17β(H)-21α(H)-30-norhopane, and 17α(H)-22,29,30-trisnorhopane in Lumbini (1:0.9:0.5) was most similar to diesel groundwater pumps (1:1.1:0.6).[23] Picene, a molecular marker of coal combustion, indicated the presence of coal burning (likely from brick kilns in the region), but at lower concentrations (1.0 ± 0.6 ng m^{-3}) than that observed in the Kathmandu Valley (3.5 ± 3.9 ng m^{-3}).[36]

Secondary Organic Aerosol (SOA) Tracers from Aromatic VOCs. 2,3-Dihydroxy-4-oxopentanoic acid (DHOPA, also known as T-3) is an SOA product of toluene[91] and other monoaromatic VOCs.[42,47] The OC-normalized concentrations of DHOPA during daytime were significantly higher than nighttime (Figure 4c; p = 0.03), consistent with its production via photochemical oxidation during the day[91] and removal via deposition during the night. The average concentration of DHOPA (17.8 ± 6.1 ng m^{-3}; Table 2) is comparable to the highest previously reported concentration in the world (13.1 ng m^{-3}), in the Pearl River Delta, China, during the winter of 2008.[92] The elevated DHOPA concentration in Lumbini corresponded to an elevated level of toluene observed during wintertime in the IGP region,[93,94] as was observed in the Pearl River Delta region in China,[95] whereas lower concentrations of DHOPA compared to the level in the IGP was observed in Atlanta, GA, parallel to a lower level of toluene concentration.[37]

The benzene dicarboxylic acids, phthalic acid, and 4-methylphthalic acid can be used as SOA tracers for naphthalene and methylnaphthalene, respectively, in the absence of appreciable primary sources.[42,48,96] Neither compound correlated significantly with hopanes and levoglucosan, while both compounds (Figure 4c, Table S4) strongly correlated with DHOPA, thus suggesting diaromatic VOC-derived SOA in Lumbini. In addition, two nitrophenols (NPs), 4NP and 2 M-4NP, were consistently detected in Lumbini (Table 2, Figure 4d). These two NPs were strongly intercorrelated, but not strongly correlated with other NACs

https://dx.doi.org/10.1021/acsearthspacechem.0c00269
ACS Earth Space Chem. 2021, 5, 226−238

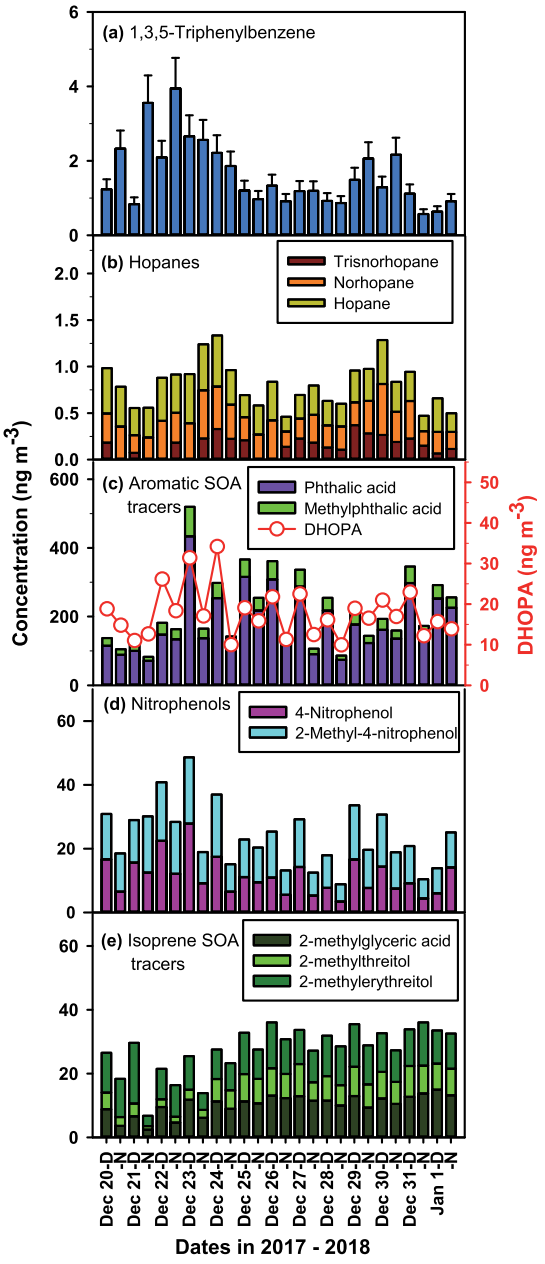

Figure 4. Time series of molecular markers from primary emission sources and secondary organic aerosols during the winter of 2017–2018 in Lumbini: (a) 1,3,5-triphenylbenzene from plastic burning, (b) hopanes from fossil fuel combustion, (c) diaromatic SOA tracers, (d), nitrophenols from SOA derived from monoaromatic VOC, and (e) isoprene SOA tracers.

(Table S3), suggesting a nonbiomass burning source. Instead, its strong correlation with DHOPA (a known tracer for toluene photooxidation) suggests photooxidation of monoaromatic compounds[73,74,97] and its strong correlation with hopane suggests SOA generated from emissions associated with fossil fuel combustion (Table S4).[98] Together, these compounds indicate the presence of SOA derived from mono and diaromatic VOC in Lumbini, which are likely to originate from biomass burning, garbage burning, and traffic-related VOC emissions, based on $PM_{2.5}$ organic carbon source apportionment (as described in Primary Source Contributions to PM2.5 OC section) and prior studies of VOC sources in the IGP and Kathmandu Valley.[34,35,93]

SOA Tracers Derived from Isoprene, Monoterpenes, and Sesquiterpenes. Tracers for SOA derived from isoprene, monoterpene, and sesquiterpene were detected consistently (Figure 4e, Figure S4). Overall, the concentrations of isoprene-derived SOA tracers were low compared to their concentrations during summer and late summer seasons in Nepal[21] and in the southeastern USA.[47] Among the isoprene tracers, 2-methylglyceric acid, formed under higher NO_x conditions,[99] was more abundant than the sum of 2-methylthreitol, and 2-methylerythritol, formed under lower NO_x conditions, by an average ratio of 1.6. This predominance of 2-methylglyceric acid has been previously observed in the Kathmandu Valley[21] and other urban sites[100] and may reflect a relatively large influence of NO_x on isoprene SOA formation in Lumbini, where the NO_x level (approximately 8.0 ppbv) was similar to the NO_x level observed in urban areas of the IGP.[101] Notably, isoprene observed in the IGP and Kathmandu Valley in wintertime has been mainly attributed to traffic and biomass burning,[34,35,93] rather than biogenic emissions. Two of ten monoterpene SOA tracers were detected in Lumbini, 3-hydroxyglutaric acid and 3-acetyladepic acid (Figure S4a, Table 2), while the remaining were below the method detection limit. The sesquiterpene SOA tracer β-caryophyllinic acid[102] was detected in every sample throughout the study period (Figure S4b, Table 2). In comparison to the Kathmandu Valley, wintertime levels of isoprene, monoterpene, and sesquiterpene SOA tracers in Lumbini were higher than the premonsoon season[36] but comparable to or less than those in the postmonsoon season.[21]

Source Apportionment of $PM_{2.5}$ OC. $PM_{2.5}$ OC in Lumbini was apportioned to six primary sources (garbage burning, dung burning, other biomass burning, gasoline engines, diesel engines, and coal combustion) using CMB modeling and seven secondary sources (isoprene SOA, monoterpene SOA, sesquiterpene SOA, toluene SOA, naphthalene SOA, methylnaphthalene SOA, and cresol SOA) using the SOA tracer method.[47] Our best estimate of sources of $PM_{2.5}$ OC (our "base case" scenario) utilizes regional source profiles when possible (see CMB Modeling in the Methods section). For the base case model result, the other biomass burning profile corresponded to open burning of twigs and dung sampled in Lumbini.[23] On average, CMB apportioned 52 ± 13% of OC to primary sources and 19 ± 5% of OC to secondary sources with the remaining 30 ± 10% of OC unapportioned and referred to as having "other sources" (Figure 5, Table 3). These other sources may be cooking with nonbiomass fuels (e.g., LPG), mixed industrial emissions, resuspended dust, or other uncharacterized primary and secondary sources. Unapportioned OC can also arise from an underestimation of primary source emissions and SOA contributions. The unapportioned OC during daytime (34%) was significantly higher than nighttime (26%), suggesting that SOA was a major part of the unapportioned OC especially during the day. The CMB model did not converge on December 20-N, so primary source contributions are not reported.

Primary Source Contributions to $PM_{2.5}$ OC. Dung and other biomass burning (e.g., crop residues, wood) was the largest contributor to $PM_{2.5}$ OC (Table 3). Dung burning contributed 3 to 59% (24 ± 16% on average) of $PM_{2.5}$ OC, while open biomass burning contributed 8 to 29% (20 ± 7% on average). Likely sources of biomass burning include wood and dung burning for household cooking, open biomass fires

https://dx.doi.org/10.1021/acsearthspacechem.0c00269
ACS Earth Space Chem. 2021, 5, 226–238

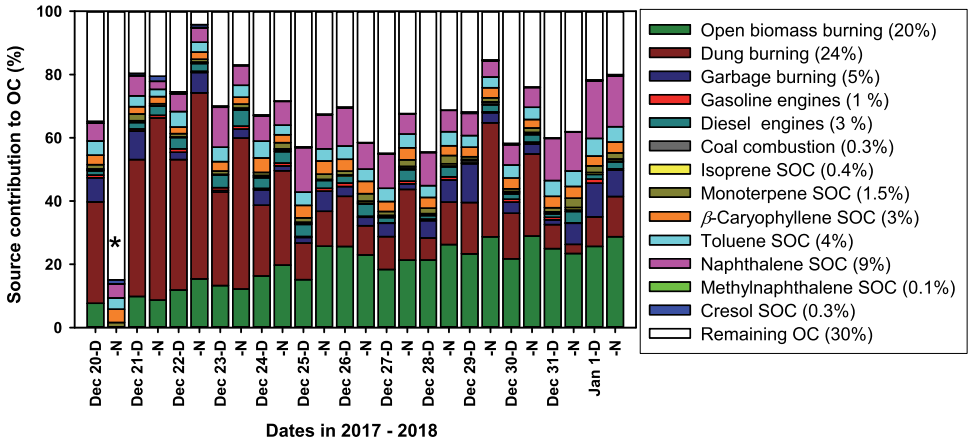

Figure 5. Apportionment of $PM_{2.5}$ OC to its primary and secondary sources by CMB modeling. Values in parentheses are average percent contributions by the corresponding sources. The CMB model did not converge to a stable solution for primary sources on December 20-N and is marked with a star.

Table 3. Absolute and Relative Primary and Secondary Source Contributions to $PM_{2.5}$ OC in Lumbini[a]

		relative contribution (%)			
sources	absolute contribution (μgC m^{-3})	overall	day	night	p-value
dung burning	14.7 ± 12.0	23.5 ± 16.1	20.1 ± 12.6	27.3 ± 19.1	0.23
open biomass burning	10.5 ± 3.9	19.9 ± 6.6	18.1 ± 6.2	21.8 ± 6.7	0.27
garbage/plastic burning	2.7 ± 2.2	4.7 ± 3.2	5.2 ± 3.7	4.2 ± 2.7	0.57
diesel engines	1.4 ± 0.9	2.6 ± 1.2	2.1 ± 1.2	3.1 ± 0.9	0.04*
gasoline engines	0.37 ± 0.22	0.66 ± 0.35	0.69 ± 0.40	0.63 ± 0.30	0.74
coal combustion	0.16 ± 0.14	0.30 ± 0.22	0.25 ± 0.22	0.36 ± 0.21	0.23
isoprene SOC	0.18 ± 0.05	0.36 ± 0.16	0.35 ± 0.11	0.38 ± 0.21	0.65
monoterpene SOC	0.77 ± 0.10	1.5 ± 0.6	1.3 ± 0.4	1.7 ± 0.7	0.08
sesquiterpene SOC	1.77 ± 0.64	3.2 ± 0.7	3.3 ± 0.7	3.2 ± 0.7	0.80
toluene SOC	2.3 ± 0.8	4.1 ± 0.8	4.4 ± 0.6	3.8 ± 0.8	0.03*
naphthalene SOC	4.7 ± 2.4	8.7 ± 3.9	10.0 ± 3.9	7.5 ± 3.6	0.10
methylnaphthalene SOC	0.07 ± 0.03	0.12 ± 0.05	0.15 ± 0.04	0.10 ± 0.04	0.01*
cresol SOC	0.15 ± 0.24	0.25 ± 0.36	0.18 ± 0.17	0.32 ± 0.49	0.44
other OC	16.4 ± 7.5	29.8 ± 10.3	33.9 ± 8.5	25.4 ± 10.6	0.048*

[a]Percent contributions of the sources during day and night periods were compared and p-values <0.05 (highlighted with an asterisk) indicate significant differences at the 95% confidence interval.

for heating, cofiring biomass with coal in brick kilns, and agricultural residue burning. The molecular markers that were used to distinguish wood or crop residue from dung burning were levoglucosan, coprostanol, and stigmastanol, with 83% of the levoglucosan attributed to biomass burning and 17% to dung burning while 100% of the coprostanol and stigmastanol was apportioned to dung burning. Temporally, the relative contribution of dung burning was higher in the early part of the study, consistent with the time-varying trend in stigmastanol (Figure 2a).

Garbage is commonly burned in open fires in South Asia,[38] although there are few estimates of regional emissions from this source[103] and its impact on air quality.[17,36,38,86,104] To the best of our knowledge, this is the first measurement of TPB in Lumbini and the first particle-phase tracer-based estimate of garbage burning contribution to air quality in the IGP. The plastic/garbage burning contribution to $PM_{2.5}$ OC ranged from 0.6 to 12% and averaged 4.7 ± 3.2% (Table 3). The garbage burning contribution to $PM_{2.5}$ OC in Lumbini was approximately four times lower than the contribution of this source at an urban site in the Kathmandu Valley[36] and three times lower than its contribution in the National Capital Region (NCR) of India.[17] Owing to its sizable contribution to $PM_{2.5}$ OC (reaching up to 12%), garbage burning should be considered in future $PM_{2.5}$ source apportionment studies in South Asia.

$PM_{2.5}$ OC was apportioned to three types of fossil fuel combustion: diesel engines (0.25 to 5.1%), gasoline engines (0.16 to 1.3%), and coal combustion (0.11 to 0.74%), (Table 3). Some of the likely contributors to the diesel engine sources are groundwater pumps that are used in the region for irrigation and agricultural equipment (i.e., tractors) fueled by diesel. In comparison to the 23% contribution at an urban site in Kathmandu,[36] the average impact of fossil fuels on $PM_{2.5}$ OC in Lumbini (3.6%) was small. In addition, in comparison to biomass burning in Lumbini, the estimated primary emissions from fossil fuel use were relatively small.

Secondary Source Contribution to $PM_{2.5}$ OC. The SOA tracer method introduced by Kleindienst et al.[47] was used to estimate the secondary organic carbon (SOC) contribution by VOC precursors to SOA in Lumbini (Table 3). The tracer-to-OC values used in the calculation of SOC are summarized in the Supporting Information Table S5. The contribution of cresols emitted from biomass burning to SOA was estimated via NACs to be 0.15 ± 0.24 μgC m^{-3} contributing 0.25 ± 0.36% of $PM_{2.5}$ OC. This partial biomass burning (BB)-SOA contribution to OC in Lumbini is comparable to the contribution of this source in Atlanta, GA, during winter (0.27%),[37] which is the only previous SOA tracer method estimation for this source. Although this represents only a small fraction of BB-SOA, these data demonstrate the

https://dx.doi.org/10.1021/acsearthspacechem.0c00269
ACS Earth Space Chem. 2021, 5, 226−238

conversion of gases emitted from biomass burning to SOA in a region heavily impacted by biomass burning. Mono- and diaromatic VOCs that are emitted from vehicles, biomass burning, garbage burning, industrial emissions, and solvent use[105] contributed the most to the estimated SOA, averaging 7.0 ± 3.0 μgC m^{-3} and 13.0 ± 4.5% of $PM_{2.5}$ OC, respectively. Isoprene SOA contributions to $PM_{2.5}$ OC were relatively small (averaging 0.36 ± 0.16%), compared to monoterpenes (1.5 ± 0.6%), and sesquiterpenes (3.2 ± 0.7%). These data show a predominance of SOA from combustion-derived VOC over biogenic VOC in wintertime and demonstrate an impact of biomass burning on SOA, although the full extent of the BB impact is not yet understood.

CONCLUSIONS AND ENVIRONMENTAL IMPLICATIONS

During the winter season in the IGP at Lumbini, Nepal, both $PM_{2.5}$ and PM_{10} consistently exceeded the WHO guidelines by factors of up to 12 for $PM_{2.5}$ which ranged 48−295 μg m^{-3} and PM_{10} which ranged 60−343 μg m^{-3}, indicating very poor air quality. The concentrations of the fresh biomass burning tracer levoglucosan, the aged biomass burning tracers (NACs), and the dung burning tracer stigmastanol were among the highest concentrations ever observed in the world. The primary sources of $PM_{2.5}$ OC in Lumbini during the wintertime were dominated by biomass and dung burning (44% combined). Primary $PM_{2.5}$ OC was also influenced by fossil fuel combustion (4%) and plastic burning (5%). This study contributes to mounting evidence for the importance of garbage burning on South Asian air quality[17,23,36,38,104] that should be further examined in terms of its source emissions and ambient air quality impacts. The secondary aerosol formation was indicated by sulfate, nitrate, SOA tracers from monoaromatic and diaromatic VOCs, isoprene, and monoterpenes with aromatic precursors being dominant among the SOA precursors studied. SOC was small in comparison to primary OC from biomass burning. BB-SOA contributions to $PM_{2.5}$ were indicated by the high levels of molecular tracers of cresol-derived SOA. The product distribution of BB-SOA tracers, especially nitroaromatics, was sensitive to RH and fog processing and this was verified for the first time with field measurements. Although the cresol SOA contribution alone was a small part of total SOC, total BB-SOA is expected to be much higher considering the broader pool of VOCs (including benzene, toluene, ethylbenzene, xylene, and trimethylbenzene)[22,106] emitted from this source. An additional BB-SOA contribution is likely to contribute toward the 30 ± 10% of OC that was not apportioned. Primary BB emissions may also contribute to this, given their dominance as an OC source and the uncertainty associated with the source estimates.

This study provides a detailed examination of $PM_{2.5}$ composition and sources during a heavily polluted, 13 day period in the dry winter season of 2017-18. Because PM levels exceed WHO guidelines throughout much of the year (Figure S1), further research is needed to assess the impacts and variability of PM sources over longer time scales. Altogether, our chemical characterization and source apportionment demonstrate major biomass burning impacts on ambient $PM_{2.5}$ in the region. The second-largest contributing source sector was secondary aerosols, including ammonium nitrate, ammonium sulfate, and SOA. Although fossil fuel combustion and garbage burning contributions are small in rural areas in comparison to these, these anthropogenic sources may be more readily mitigated. Garbage burning, in particular, warrants further consideration because of its hazardous nature and opportunity for emission reductions. Substantial reductions to $PM_{2.5}$, however, must target the dominant source of biomass burning, which originates from numerous sources in the IGP, including residential use of dung and biomasses and crop residue burning.

ASSOCIATED CONTENT

Supporting Information

The Supporting Information is available free of charge at https://pubs.acs.org/doi/10.1021/acsearthspacechem.0c00269.

Day and nighttime concentrations of PM, OC, EC, and inorganic ions, Table S1; comparison of levoglucosan and NACs in Lumbini with prior studies, Table S2; correlation (r) of NACs with levoglucosan and other NACs, Table S3; day and nighttime concentrations of organic molecular markers, Table S4; concentrations of PAHs, Table S5; correlation (r) of benzene dicarboxylic acids and nitrophenols with DHOPA, hopane, and levoglucosan, Table S6; tracer-to-OC ratios for SOA derived from selected VOC precursors, Table S7; 24 h $PM_{2.5}$ concentrations measured at the Lumbini Air Quality Monitoring Station from January 2017 to September 2018, Figure S1; visibility at Kathmandu and Lucknow, Figure S2; hourly time-series plot for temperature, relative humidity, and radiation, and wind speed and direction during the sampling period in winter 2017−2018 at Lumbini, Figure S3; and time series of SOA tracers from monoterpene and sesquiterpene, Figure S4 (PDF)

AUTHOR INFORMATION

Corresponding Author

Elizabeth A. Stone − *Department of Chemistry and Department of Chemical and Biochemical Engineering, University of Iowa, Iowa City, Iowa 52242, United States*; Email: betsy-stone@uiowa.edu

Authors

Md. Robiul Islam − *Department of Chemistry, University of Iowa, Iowa City, Iowa 52242, United States*

Tianyi Li − *Department of Chemistry, University of Iowa, Iowa City, Iowa 52242, United States*

Khadak Mahata − *Alpine Consultancy, Kathmandu 44600, Nepal*

Nita Khanal − *Alpine Consultancy, Kathmandu 44600, Nepal*

Benjamin Werden − *Department of Environmental Health and Engineering, Johns Hopkins University, Baltimore, Maryland 21205, United States*

Michael R. Giordano − *OSU-EFLUVE, LISA-CNRS, UPEC, Créteil 94000, France*

P. S. Praveen − *International Centre for Integrated Mountain Development (ICIMOD), Kathmandu 44700, Nepal*

Narayan Babu Dhital − *Tribhuvan University, Kathmandu 44700, Nepal*

Anobha Gurung − *Clean Cooking Alliance, Washington, D. C. 20006, United States*

Arnico K. Panday − *International Centre for Integrated Mountain Development (ICIMOD), Kathmandu 44700, Nepal*

https://dx.doi.org/10.1021/acsearthspacechem.0c00269
ACS Earth Space Chem. 2021, 5, 226−238

Indu Bikram Joshi − *Department of Environment, Ministry of Forests and Environment, Kathmandu 44600, Nepal*
Shankar Prasad Poudel − *Department of Environment, Ministry of Forests and Environment, Kathmandu 44600, Nepal*
Yanbo Wang − *Department of Computer Science, Emory College of Arts and Sciences, Atlanta, Georgia 30322, United States*
Eri Saikawa − *Department of Environmental Sciences, Emory University, Atlanta, Georgia 30322, United States;* orcid.org/0000-0003-3166-8620
Robert J. Yokelson − *Department of Chemistry, University of Montana, Missoula, Montana 59812, United States*
Peter F. DeCarlo − *Department of Environmental Health and Engineering, Johns Hopkins University, Baltimore, Maryland 21205, United States;* orcid.org/0000-0001-6385-7149

Complete contact information is available at: https://pubs.acs.org/10.1021/acsearthspacechem.0c00269

Funding

This project was funded by the National Science Foundation through the grant entitled "Collaborative Research: Measurements of Selected Combustion Emissions in Nepal and Bhutan Integrated with Source Apportionment and Chemical Transport Modeling for South Asia" via award numbers AGS-1351616 to the University of Iowa, AGS-1349976 to the University of Montana, AGS-1350021 to Emory University, and AGS-1461458 to Drexel University. NAMaSTE 2 was partially supported by core funds of ICIMOD contributed by the governments of Afghanistan, Australia, Austria, Bangladesh, Bhutan, China, India, Myanmar, Nepal, Norway, Pakistan, Switzerland, and the United Kingdom, as well as by funds from the Government of Sweden to ICIMOD's Atmosphere Initiative.

Notes

The authors declare no competing financial interest.
All filter-based PM measurements with analytical uncertainties and CMB model results with standard errors are available for download at https://doi.org/10.17605/OSF.IO/S2WE.[107]

REFERENCES

(1) Ramanathan, V.; Li, F.; Ramana, M.; Praveen, P.; Kim, D.; Corrigan, C.; Nguyen, H.; Stone, E. A.; Schauer, J. J.; Carmichael, G. Atmospheric brown clouds: Hemispherical and regional variations in long-range transport, absorption, and radiative forcing. *J. Geophys. Res.: Atmos.* **2007**, *112*, No. D008124.
(2) Manandhar, K., The fog episode in southern Terai plains of Nepal: some observations and concepts. *J. Hydrol. Meteorol.*. 2006, *3* (1).
(3) Shrestha, S.; Moore, G. A.; Peel, M. C. Trends in winter fog events in the Terai region of Nepal. *Agri. and Forest Meteorol.* **2018**, *259*, 118−130.
(4) Ramanathan, V.; Ramana, M. V. Persistent, widespread, and strongly absorbing haze over the Himalayan foothills and the Indo-Gangetic Plains. *Pure and Appl. Geophys.* **2005**, *162*, 1609−1626.
(5) Rupakheti, D.; Adhikary, B.; Praveen, P. S.; Rupakheti, M.; Kang, S. C.; Mahata, K. S.; Naja, M.; Zhang, Q. G.; Panday, A. K.; Lawrence, M. G. Pre-monsoon air quality over Lumbini, a world heritage site along the Himalayan foothills. *Atmos. Chem. Phys.* **2017**, *17*, 11041−11063.
(6) Chen, P.; Li, C.; Kang, S.; Yan, F.; Zhang, Q.; Ji, Z.; Tripathee, L.; Rupakheti, D.; Rupakheti, M.; Qu, B. Source apportionment of particle-bound polycyclic aromatic hydrocarbons in Lumbini, Nepal by using the positive matrix factorization receptor model. *Atmos. Res.* **2016**, *182*, 46−53.
(7) Chen, P. F.; Kang, S. C.; Tripathee, L.; Panday, A. K.; Rupakheti, M.; Rupakheti, D.; Zhang, Q. G.; Guo, J. M.; Li, C. L.; Pu, T. Severe air pollution and characteristics of light-absorbing particles in a typical rural area of the Indo-Gangetic Plain. *Environ. Sci. Pollut. Res.* **2020**, *27*, 10617−10628.
(8) Tripathee, L.; Kang, S. C.; Rupakheti, D.; Cong, Z. Y.; Zhang, Q. G.; Huang, J. Chemical characteristics of soluble aerosols over the central Himalayas: insights into spatiotemporal variations and sources. *Environ. Sci. Pollut. Res.* **2017**, *24*, 24454−24472.
(9) Wan, X.; Kang, S.; Li, Q.; Rupakheti, D.; Zhang, Q.; Guo, J.; Chen, P.; Tripathee, L.; Rupakheti, M.; Panday, A. K. Organic molecular tracers in the atmospheric aerosols from Lumbini, Nepal, in the northern Indo-Gangetic Plain: influence of biomass burning. *Atmos. Chem. Phys.* **2017**, *17*, 8867−8885.
(10) Maji, S.; Ghosh, S.; Ahmed, S. Association of air quality with respiratory and cardiovascular morbidity rate in Delhi. *India. Int. J. Environ. Health Res.* **2018**, *28*, 471−490.
(11) Forouzanfar, M. H.; Alexander, L.; Anderson, H. R.; Bachman, V. F.; Biryukov, S.; Brauer, M.; Burnett, R.; Casey, D.; Coates, M. M.; Cohen, A. Global, regional, and national comparative risk assessment of 79 behavioural, environmental and occupational, and metabolic risks or clusters of risks in 188 countries, 1990−2013: a systematic analysis for the Global Burden of Disease Study 2013. *Lancet* **2015**, *386*, 2287−2323.
(12) Ray, D.; Ghosh, A.; Chatterjee, A.; Ghosh, S. K.; Raha, S. Size-specific PAHs and Associated Health Risks over a Tropical Urban Metropolis: Role of Long-range Transport and Meteorology. *Aerosol Air Qual. Res.* **2019**, *19*, 2446−2463.
(13) Agarwal, N. K.; Sharma, P.; Agarwal, S. K. Particulate matter air pollution and cardiovascular disease. *Med. Sci.* **2010**, *121*, 2331−2378.
(14) Rajeev, P.; Rajput, P.; Singh, D. K.; Singh, A. K.; Gupta, T. Risk assessment of submicron PM-bound hexavalent chromium during wintertime. *Hum. Ecol. Risk Assess.* **2018**, *24*, 1453−1463.
(15) Neupane, B.; Chen, P. F.; Kang, S. C.; Tripathee, L.; Rupakheti, D.; Sharma, C. M. Health risk assessment of atmospheric polycyclic aromatic hydrocarbons over the Central Himalayas. *Hum. Ecol. Risk Assess.* **2018**, *24*, 1969−1982.
(16) Liu, T. J.; Marlier, M. E.; DeFries, R. S.; Westervelt, D. M.; Xia, K. R.; Fiore, A. M.; Mickley, L. J.; Cusworth, D. H.; Milly, G. Seasonal impact of regional outdoor biomass burning on air pollution in three Indian cities: Delhi, Bengaluru, and Pune. *Atmos. Environ.* **2018**, *172*, 83−92.
(17) Gadi, R.; Shivani; Sharma, S. K.; Mandal, T. K. Source apportionment and health risk assessment of organic constituents in fine ambient aerosols (PM2.5): A complete year study over National Capital Region of India. *Chemosphere* **2019**, *221*, 583−596.
(18) Simoneit, B. R. T.; Schauer, J. J.; Nolte, C. G.; Oros, D. R.; Elias, V. O.; Fraser, M. P.; Rogge, W. F.; Cass, G. R. Levoglucosan, a tracer for cellulose in biomass burning and atmospheric particles. *Atmos. Environ.* **1999**, *33*, 173−182.
(19) Ali, K.; Trivedi, D. K.; Chate, D. M.; Beig, G.; Acharja, P.; Trimbake, H. K. PM2.5, PM10 and surface ozone over Lumbini Protected Zone, Nepal, during monsoon season of 2012. *J. Earth Syst. Sci.* **2019**, *128*, No. 0088.
(20) Stone, E. A.; Schauer, J. J.; Pradhan, B. B.; Dangol, P. M.; Habib, G.; Venkataraman, C.; Ramanathan, V. Characterization of emissions from South Asian biofuels and application to source apportionment of carbonaceous aerosol in the Himalayas. *J.Geophys. Res.* **2010**, *115*, D06301.
(21) Stone, E. A.; Nguyen, T. T.; Pradhan, B. B.; Dangol, P. M. Assessment of biogenic secondary organic aerosol in the Himalayas. *Environ. Chem.* **2012**, *9*, 263−272.
(22) Stockwell, C. E.; Christian, T. J.; Goetz, J. D.; Jayarathne, T.; Bhave, P. V.; Praveen, P. S.; Adhikari, S.; Maharjan, R.; DeCarlo, P. F.; Stone, E. A.; Saikawa, E.; Blake, D. R.; Simpson, I.; Yokelson, R. J.; Panday, A. K. Nepal Ambient Monitoring and Source Testing Experiment (NAMaSTE): Emissions of trace gases and light-

absorbing carbon from wood and dung cooking fires, garbage and crop residue burning, brick kilns, and other sources. *Atmos. Chem. Phys.* **2016**, *16*, 11043−11081.
(23) Jayarathne, T.; Stockwell, C. E.; Bhave, P. V.; Praveen, P. S.; Rathnayake, C. M.; Islam, M. R.; Panday, A. K.; Adhikari, S.; Maharjan, R.; Goetz, J. D.; DeCarlo, P. F.; Saikawa, E.; Yokelson, R. J.; Stone, E. A. Nepal Ambient Monitoring and Source Testing Experiment (NAMaSTE): emissions of particulate matter from wood- and dung-fueled cooking fires, garbage and crop residue burning, brick kilns, and other sources. *Atmos. Chem. Phys.* **2018**, *18*, 2259−2286.
(24) Pattanayak, S. K.; Yang, J. C.; Whittington, D.; Bal Kumar, K. Coping with unreliable public water supplies: averting expenditures by households in Kathmandu, Nepal. *Water Resour. Res.* **2005**, *41*, No. W02012.
(25) Pokhrel, A. K.; Bates, M. N.; Acharya, J.; Valentiner-Branth, P.; Chandyo, R. K.; Shrestha, P. S.; Raut, A. K.; Smith, K. R. J. A. E. PM2.5 in household kitchens of Bhaktapur, Nepal, using four different cooking fuels. *Atmos. Environ.* **2015**, *113*, 159−168.
(26) Yevich, R.; Logan, J. A. An assessment of biofuel use and burning of agricultural waste in the developing world. *Global Biogeochem. Cycles* **2003**, *17*, 1095.
(27) Maithel, S.; Lalchandani, D.; Malhotra, G.; Bhanware, P.; Uma, R.; Ragavan, S.; Athalye, V., Brick Kilns Performance Assessment: A Roadmap for Cleaner Brick Production in India. *A Shakti sustainable energy foundation climate works Foundation supported initiative, report*; 2012.
(28) Safai, P. D.; Kewat, S.; Pandithurai, G.; Praveen, P. S.; Ali, K.; Tiwari, S.; Rao, P. S. P.; Budhawant, K. B.; Saha, S. K.; Devara, P. C. S. Aerosol characteristics during winter fog at Agra, North India. *J. Atmos. Chem.* **2008**, *61*, 101−118.
(29) Ram, K.; Sarin, M.; Sudheer, A.; Rengarajan, R. Carbonaceous and secondary inorganic aerosols during wintertime fog and haze over urban sites in the Indo-Gangetic Plain. *Aerosol Air Qual. Res.* **2012**, *12*, 359−370.
(30) Aneja, V. P.; Schlesinger, W. H.; Erisman, J. W.; Behera, S. N.; Sharma, M.; Battye, W. Reactive nitrogen emissions from crop and livestock farming in India. *Atmos. Environ.* **2012**, *47*, 92−103.
(31) Fowler, D.; Flechard, C.; Skiba, U.; Coyle, M.; Cape, J. N. The atmospheric budget of oxidized nitrogen and its role in ozone formation and deposition. *New Phytol.* **1998**, *139*, 11−23.
(32) Jena, C.; Ghude, S. D.; Beig, G.; Chate, D. M.; Kumar, R.; Pfister, G. G.; Lal, D. M.; Surendran, D. E.; Fadnavis, S.; van der RJ, A. Inter-comparison of different NOX emission inventories and associated variation in simulated surface ozone in Indian region. *Atmos. Environ.* **2015**, *117*, 61−73.
(33) Suneja, J.; Kotnala, G.; Kaur, A.; Mandal, T. K.; Sharma, S. K. Long-Term Measurements of SO2 Over Delhi, India. *MAPAN-J. Metrol. Soc. India* **2020**, *35*, 125−133.
(34) Sarkar, C.; Sinha, V.; Kumar, V.; Rupakheti, M.; Panday, A.; Mahata, K. S.; Rupakheti, D.; Kathayat, B.; Lawrence, M. G. Overview of VOC emissions and chemistry from PTR-TOF-MS measurements during the SusKat-ABC campaign: high acetaldehyde, isoprene and isocyanic acid in wintertime air of the Kathmandu Valley. *Atmos. Chem. Phys.* **2016**, *16*, 3979−4003.
(35) Sarkar, C.; Sinha, V.; Sinha, B.; Panday, A. K.; Rupakheti, M.; Lawrence, M. G. Source apportionment of NMVOCs in the Kathmandu Valley during the SusKat-ABC international field campaign using positive matrix factorization. *Atmos. Chem. Phys.* **2017**, *17*, 8129−8156.
(36) Islam, M. R.; Jayarathne, T.; Simpson, I. J.; Werden, B.; Maben, J.; Gilbert, A.; Praveen, P. S.; Adhikari, S.; Panday, A. K.; Rupakheti, M.; Blake, D. R.; Yokelson, R. J.; DeCarlo, P. F.; Keene, W. C.; Stone, E. A. Ambient air quality in the Kathmandu Valley, Nepal, during the pre-monsoon: concentrations and sources of particulate matter and trace gases. *Atmos. Chem. Phys.* **2020**, *20*, 2927−2951.
(37) Al-Naiema, I. M.; Offenberg, J. H.; Madler, C. J.; Lewandowski, M.; Kettler, J.; Fang, T.; Stone, E. A. Secondary organic aerosols from aromatic hydrocarbons and their contribution to fine particulate matter in Atlanta, Georgia. *Atmos. Environ.* **2020**, *223*, 117227.
(38) Wiedinmyer, C.; Yokelson, R. J.; Gullett, B. K. Global emissions of trace gases, particulate matter, and hazardous air pollutants from open burning of domestic waste. *Environ. Sci. Technol.* **2014**, *48*, 9523−9530.
(39) Simoneit, B. R. T.; Medeiros, P. M.; Didyk, B. M. Combustion products of plastics as indicators for refuse burning in the atmosphere. *Environ. Sci. Technol.* **2005**, *39*, 6961−6970.
(40) Schauer, J. J.; Mader, B. T.; Deminter, J. T.; Heidemann, G.; Bae, M. S.; Seinfeld, J. H.; Flagan, R. C.; Cary, R. A.; Smith, D.; Huebert, B. J.; Bertram, T.; Howell, S.; Kline, J. T.; Quinn, P.; Bates, T.; Turpin, B.; Lim, H. J.; Yu, J. Z.; Yang, H.; Keywood, M. D. ACE-Asia intercomparison of a thermal-optical method for the determination of particle-phase organic and elemental carbon. *Environ. Sci. Technol.* **2003**, *37*, 993−1001.
(41) Nolte, C. G.; Schauer, J. J.; Cass, G. R.; Simoneit, B. R. Trimethylsilyl derivatives of organic compounds in source samples and in atmospheric fine particulate matter. *Environ. Sci. Technol.* **2002**, *36*, 4273−4281.
(42) Al-Naiema, I. M.; Stone, E. A. Evaluation of anthropogenic secondary organic aerosol tracers from aromatic hydrocarbons. *Atmos. Chem. Phys.* **2017**, *17*, 2053−2065.
(43) Jayarathne, T.; Stockwell, C. E.; Yokelson, R. J.; Nakao, S.; Stone, E. A. Emissions of fine particle fluoride from biomass burning. *Environ. Sci. Technol.* **2014**, *48*, 12636−12644.
(44) Schauer, J. J.; Kleeman, M. J.; Cass, G. R.; Simoneit, B. R. Measurement of emissions from air pollution sources. 5. C1− C32 organic compounds from gasoline-powered motor vehicles. *Environ. Sci. Technol.* **2002**, *36*, 1169−1180.
(45) Lough, G. C.; Christensen, C. G.; Schauer, J. J.; Tortorelli, J.; Mani, E.; Lawson, D. R.; Clark, N. N.; Gabele, P. A. Development of molecular marker source profiles for emissions from on-road gasoline and diesel vehicle fleets. *J. Air Waste Manage. Assoc.* **2012**, *57*, 1190−1199.
(46) Zhang, Y.; Schauer, J. J.; Zhang, Y.; Zeng, L.; Wei, Y.; Liu, Y.; Shao, M. Characteristics of particulate carbon emissions from real-world Chinese coal combustion. *Environ. sci. Technol.* **2008**, *42*, 5068−5073.
(47) Kleindienst, T. E.; Jaoui, M.; Lewandowski, M.; Offenberg, J. H.; Lewis, C. W.; Bhave, P. V.; Edney, E. O. Estimates of the contributions of biogenic and anthropogenic hydrocarbons to secondary organic aerosol at a southeastern US location. *Atmos. Environ.* **2007**, *41*, 8288−8300.
(48) Kleindienst, T.; Jaoui, M.; Lewandowski, M.; Offenberg, J.; Docherty, K. The formation of SOA and chemical tracer compounds from the photooxidation of naphthalene and its methyl analogs in the presence and absence of nitrogen oxides. *Atmos. Chem. Phys.* **2012**, *12*, 8711−8726.
(49) Hewett, P.; Ganser, G. H. A comparison of several methods for analyzing censored data. *Ann.Occup. Hyg.* **2007**, *51*, 611−632.
(50) Schauer, J. J.; Kleeman, M. J.; Cass, G. R.; Simoneit, B. R. Measurement of emissions from air pollution sources. 3. C1-C29 organic compounds from fireplace combustion of wood. *Environ. Sci. Technol.* **2001**, *35*, 1716−1728.
(51) Hong, Y. Y.; Liu, Y. M.; Chen, X. Y.; Fan, Q.; Chen, C.; Chen, X. L.; Wang, M. J. The role of anthropogenic chlorine emission in surface ozone formation during different seasons over eastern China. *Sci. Total Environ.* **2020**, *723*, 137697.
(52) Stone, E.; Schauer, J.; Quraishi, T. A.; Mahmood, A. Chemical characterization and source apportionment of fine and coarse particulate matter in Lahore. *Pakistan. Atmos. Environ.* **2010**, *44*, 1062−1070.
(53) Simpson, W. R.; Brown, S. S.; Saiz-Lopez, A.; Thornton, J. A.; von Glasow, R. Tropospheric Halogen Chemistry: Sources, Cycling, and Impacts. *Chem. Rev.* **2015**, *115*, 4035−4062.
(54) Saxena, M.; Sharma, A.; Sen, A.; Saxena, P.; Mandal, T. K.; Sharma, S. K.; Sharma, C. Water soluble inorganic species of PM10

and PM2.5 at an urban site of Delhi, India: seasonal variability and sources. *Atmos. Res.* **2017**, *184*, 112−125.
(55) Nirmalkar, J.; Deshmukh, D. K.; Deb, M. K.; Tsai, Y. I.; Sopajaree, K. Mass loading and episodic variation of molecular markers in PM2.5 aerosols over a rural area in eastern central India. *Atmos. Environ.* **2015**, *117*, 41−50.
(56) Li, J. J.; Wang, G. H.; Aggarwal, S. G.; Huang, Y.; Ren, Y. Q.; Zhou, B. H.; Singh, K.; Gupta, P. K.; Cao, J. J.; Zhang, R. Comparison of abundances, compositions and sources of elements, inorganic ions and organic compounds in atmospheric aerosols from Xi'an and New Delhi, two megacities in China and India. *Sci. Total Environ.* **2014**, *476-477*, 485−495.
(57) Singh, N.; Banerjee, T.; Murari, V.; Deboudt, K.; Khan, M. F.; Singh, R.; Latif, M. T. Insights into size-segregated particulate chemistry and sources in urban environment over central Indo-Gangetic Plain. *Chemosphere* **2020**, *263*, 128030.
(58) Sorathia, F.; Rajput, P.; Gupta, T. Dicarboxylic acids and levoglucosan in aerosols from Indo-Gangetic Plain: Inferences from day night variability during wintertime. *Sci. Total Environ.* **2018**, *624*, 451−460.
(59) Simoneit, B. R. T. Biomass burning - A review of organic tracers for smoke from incomplete combustion. *Appl. Geochem.* **2002**, *17*, 129−162.
(60) Sheesley, R. J.; Schauer, J. J.; Chowdhury, Z.; Cass, G. R.; Simoneit, B. R. Characterization of organic aerosols emitted from the combustion of biomass indigenous to South Asia. *J. Geophys. Res.* **2003**, *108*, 4285.
(61) Sharma, M. *Techno-environmental assessment of biomass as a source of energy: the case of Nepal*; M. Eng. Thesis. Asian Institute of Technology: Bangkok, 1995.
(62) Iinuma, Y.; Boge, O.; Grafe, R.; Herrmann, H. Methyl-Nitrocatechols: Atmospheric Tracer Compounds for Biomass Burning Secondary Organic Aerosols. *Environ. Sci. Technol.* **2010**, *44*, 8453−8459.
(63) Kitanovski, Z.; Grgic, I.; Vermeylen, R.; Claeys, M.; Maenhaut, W. Liquid chromatography tandem mass spectrometry method for characterization of monoaromatic nitro-compounds in atmospheric particulate matter. *J. Chromatogr. A* **2012**, *1268*, 35−43.
(64) Kahnt, A.; Behrouzi, S.; Vermeylen, R.; Shalamzari, M. S.; Vercauteren, J.; Roekens, E.; Claeys, M.; Maenhaut, W. One-year study of nitro-organic compounds and their relation to wood burning in PM10 aerosol from a rural site in Belgium. *Atmos. Environ.* **2013**, *81*, 561−568.
(65) Mohr, C.; Lopez-Hilfiker, F. D.; Zotter, P.; Prevot, A. S. H.; Xu, L.; Ng, N. L.; Herndon, S. C.; Williams, L. R.; Franklin, J. P.; Zahniser, M. S.; Worsnop, D. R.; Knighton, W. B.; Aiken, A. C.; Gorkowski, K. J.; Dubey, M. K.; Allan, J. D.; Thornton, J. A. Contribution of Nitrated Phenols to Wood Burning Brown Carbon Light Absorption in Detling, United Kingdom during Winter Time. *Environ. Sci. Technol.* **2013**, *47*, 6316−6324.
(66) Zhang, Z. S.; Engling, G.; Lin, C. Y.; Chou, C. C. K.; Lung, S. C. C.; Chang, S. Y.; Fan, S. J.; Chan, C. Y.; Zhang, Y. H. Chemical speciation, transport and contribution of biomass burning smoke to ambient aerosol in Guangzhou, a mega city of China. *Atmos. Environ.* **2010**, *44*, 3187−3195.
(67) Zhang, X. L.; Lin, Y. H.; Surratt, J. D.; Weber, R. J. Sources, Composition and Absorption Angstrom Exponent of Light-absorbing Organic Components in Aerosol Extracts from the Los Angeles Basin. *Environ. Sci. Technol.* **2013**, *47*, 3685−3693.
(68) Claeys, M.; Vermeylen, R.; Yasmeen, F.; Gomez-Gonzalez, Y.; Chi, X. G.; Maenhaut, W.; Meszaros, T.; Salma, I. Chemical characterisation of humic-like substances from urban, rural and tropical biomass burning environments using liquid chromatography with UV/vis photodiode array detection and electrospray ionisation mass spectrometry. *Environ. Chem.* **2012**, *9*, 273−284.
(69) Chow, K. S.; Huang, X. H. H.; Yu, J. Z. Quantification of nitroaromatic compounds in atmospheric fine particulate matter in Hong Kong over 3 years: field measurement evidence for secondary formation derived from biomass burning emissions. *Environ. Chem.* **2016**, *13*, 665−673.
(70) Hamilton, J. F.; Webb, P. J.; Lewis, A. C.; Reviejo, M. M. Quantifying small molecules in secondary organic aerosol formed during the photo-oxidation of toluene with hydroxyl radicals. *Atmos. Environ.* **2005**, *39*, 7263−7275.
(71) Jang, M.; Kamens, R. M. Characterization of secondary aerosol from the photooxidation of toluene in the presence of NO x and 1-propene. *Environ. Sci. Technol.* **2001**, *35*, 3626−3639.
(72) Irei, S.; Rudolph, J.; Huang, L.; Auld, J.; Collin, F.; Hastie, D. Laboratory Studies of Carbon Kinetic Isotope Effects on the Production Mechanism of Particulate Phenolic Compounds Formed by Toluene Photooxidation: A Tool To Constrain Reaction Pathways. *J. Phys. Chem. A* **2014**, *119*, 5−13.
(73) Sato, K.; Takami, A.; Kato, Y.; Seta, T.; Fujitani, Y.; Hikida, T.; Shimono, A.; Imamura, T. AMS and LC/MS analyses of SOA from the photooxidation of benzene and 1,3,5-trimethylbenzene in the presence of NOx: effects of chemical structure on SOA aging. *Atmos. Chem. Phys.* **2012**, *12*, 4667−4682.
(74) Forstner, H. J. L.; Flagan, R. C.; Seinfeld, J. H. Secondary organic aerosol from the photooxidation of aromatic hydrocarbons: Molecular composition. *Environ. Sci. Technol.* **1997**, *31*, 1345−1358.
(75) Mason, S. A.; Field, R. J.; Yokelson, R. J.; Kochivar, M. A.; Tinsley, M. R.; Ward, D. E.; Hao, W. M. Complex effects arising in smoke plume simulations due to inclusion of direct emissions of oxygenated organic species from biomass combustion. *J.Geophys. Res.-Atmos.* **2001**, *106*, 12527−12539.
(76) Edye, L. A.; Richards, G. N. Analysis Of Condensates From Wood Smoke - Components Derived From Polysaccharides And Lignins. *Environ. Sci. Technol.* **1991**, *25*, 1133−1137.
(77) Nguyen, T. B.; Roach, P. J.; Laskin, J.; Laskin, A.; Nizkorodov, S. A. Effect of humidity on the composition of isoprene photooxidation secondary organic aerosol. *Atmos. Chem. Phys.* **2011**, *11*, 6931−6944.
(78) Grosjean, D. Reactions Of O-Cresol And Nitrocresol With Nox In Sunlight And With Ozone Nitrogen-Dioxide Mixtures In The Dark. *Environ. Sci. Technol.* **1985**, *19*, 968−974.
(79) Liu, J. M.; Lin, P.; Laskin, A.; Laskin, J.; Kathmann, S. M.; Wise, M.; Caylor, R.; Imholt, F.; Selimovic, V.; Shilling, J. E. Optical properties and aging of light-absorbing secondary organic aerosol. *Atmos. Chem. Phys.* **2016**, *16*, 12815−12827.
(80) Chen, P. F.; Kang, S. C.; Tripathee, L.; Ram, K.; Rupakheti, M.; Panday, A. K.; Zhang, Q.; Guo, J. M.; Wang, X. X.; Pu, T.; Li, C. L. Light absorption properties of elemental carbon (EC) and water-soluble brown carbon (WS-BrC) in the Kathmandu Valley, Nepal: A 5-year study. *Environ. Pollut.* **2020**, *261*, 114239.
(81) Izhar, S.; Gupta, T.; Panday, A. K. Improved method to apportion optical absorption by black and brown carbon under the influence of haze and fog at Lumbini, Nepal, on the Indo-Gangetic Plains. *Environ. Pollut.* **2020**, *263*, 114640.
(82) Kirillova, E. N.; Andersson, A.; Tiwari, S.; Srivastava, A. K.; Bisht, D. S.; Gustafsson, O. Water-soluble organic carbon aerosols during a full New Delhi winter: Isotope-based source apportionment and optical properties. *J.Geophys. Res.-Atmos.* **2014**, *119*, 3476−3485.
(83) Laskin, A.; Laskin, J.; Nizkorodov, S. A. Chemistry of Atmospheric Brown Carbon. *Chem. Rev.* **2015**, *115*, 4335−4382.
(84) Xie, M. J.; Chen, X.; Hays, M. D.; Lewandowski, M.; Offenberg, J.; Kleindienst, T. E.; Holder, A. L. Light Absorption of Secondary Organic Aerosol: Composition and Contribution of Nitroaromatic Compounds. *Environ. Sci. Technol.* **2017**, *51*, 11607−11616.
(85) Gu, Z.; Feng, J.; Han, W.; Wu, M.; Fu, J.; Sheng, G. Characteristics of organic matter in PM2.5 from an e-waste dismantling area in Taizhou, China. *Chemosphere* **2010**, *80*, 800−806.
(86) Fu, P. Q.; Kawamura, K.; Pavuluri, C. M.; Swaminathan, T.; Chen, J. Molecular characterization of urban organic aerosol in tropical India: contributions of primary emissions and secondary photooxidation. *Atmos. Chem. Phys.* **2010**, *10*, 2663−2689.
(87) Haque, M. M.; Kawamura, K.; Deshmukh, D. K.; Fang, C.; Song, W. H.; Bao, M. Y.; Zhang, Y. L. Characterization of organic

aerosols from a Chinese megacity during winter: predominance of fossil fuel combustion. *Atmos. Chem. Phys.* **2019**, *19*, 5147−5164.
(88) Chowdhury, Z.; Zheng, M.; Schauer, J. J.; Sheesley, R. J.; Salmon, L. G.; Cass, G. R.; Russell, A. G. Speciation of ambient fine organic carbon particles and source apportionment of PM2. 5 in Indian cities. *J. Geophys. Res.: Atmos.* **2007**, *112*, No. D008386.
(89) Shah, T., Climate change and groundwater: India's opportunities for mitigation and adaptation. *Environ. Res. Lett.* 2009, *4* (3), DOI: 10.1088/1748-9326/4/3/035005.
(90) Mukherji, A.; Rawat, S.; Shah, T. Major insights from India's minor irrigation censuses: 1986-87 to 2006-07. *Eco. and Pol. Weekly* **2013**, 115−124.
(91) Kleindienst, T.; Conver, T.; McIver, C.; Edney, E. Determination of secondary organic aerosol products from the photooxidation of toluene and their implications in ambient PM2. 5. *J. Atmos. Chem.* **2004**, *47*, 79−100.
(92) Ding, X.; Wang, X. M.; Gao, B.; Fu, X. X.; He, Q. F.; Zhao, X. Y.; Yu, J. Z.; Zheng, M. Tracer-based estimation of secondary organic carbon in the Pearl River Delta, south China. *J. Geophys. Res.: Atmos.* **2012**, *117*, No. D016596.
(93) Sahu, L. K.; Saxena, P. High time and mass resolved PTR-TOF-MS measurements of VOCs at an urban site of India during winter: Role of anthropogenic, biomass burning, biogenic and photochemical sources. *Atmos. Res.* **2015**, *164*, 84−94.
(94) Sahu, L. K.; Yadav, R.; Pal, D. Source identification of VOCs at an urban site of western India: Effect of marathon events and anthropogenic emissions. *J. Geophys. Res.-Atmos.* **2016**, *121*, 2416−2433.
(95) Chan, L. Y.; Chu, K. W.; Zou, S. C.; Chan, C. Y.; Wang, X. M.; Barletta, B.; Blake, D. R.; Guo, H.; Tsai, W. Y. Characteristics of nonmethane hydrocarbons (NMHCs) in industrial, industrial-urban, and industrial-suburban atmospheres of the Pearl River Delta (PRD) region of south China. *J. Geophys. Res.-Atmos.* **2006**, *111*, D006481.
(96) Fine, P. M.; Chakrabarti, B.; Krudysz, M.; Schauer, J. J.; Sioutas, C. Diurnal variations of individual organic compound constituents of ultrafine and accumulation mode particulate matter in the Los Angeles basin. *Environ. Sci. Technol.* **2004**, *38*, 1296−1304.
(97) Harrison, M. A. J.; Barra, S.; Borghesi, D.; Vione, D.; Arsene, C.; Olariu, R. L. Nitrated phenols in the atmosphere: a review. *Atmos. Environ.* **2005**, *39*, 231−248.
(98) Tremp, J.; Mattrel, P.; Fingler, S.; Giger, W. Phenols and nitrophenols as tropospheric pollutants - emissions from automobile exhausts and phase-transfer in the atmosphere. *Water Air and Soil Pollut.* **1993**, *68*, 113−123.
(99) Surratt, J. D.; Murphy, S. M.; Kroll, J. H.; Ng, N. L.; Hildebrandt, L.; Sorooshian, A.; Szmigielski, R.; Vermeylen, R.; Maenhaut, W.; Claeys, M.; Flagan, R. C.; Seinfeld, J. H. Chemical composition of secondary organic aerosol formed from the photooxidation of isoprene. *J. Phys. Chem. A* **2006**, *110*, 9665−9690.
(100) Lewandowski, M.; Piletic, I. R.; Kleindienst, T. E.; Offenberg, J. H.; Beaver, M. R.; Jaoui, M.; Docherty, K. S.; Edney, E. O. Secondary organic aerosol characterisation at field sites across the United States during the spring-summer period. *Int. J. Environ. Anal. Chem.* **2013**, *93*, 1084−1103.
(101) Singh, S.; Kulshrestha, U. Rural versus urban gaseous inorganic reactive nitrogen in the Indo-Gangetic plains (IGP) of India. *Environ. Res. Lett.* **2014**, *9*, 125004.
(102) Jaoui, M.; Lewandowski, M.; Kleindienst, T. E.; Offenberg, J. H.; Edney, E. O. *β*-caryophyllinic acid: An atmospheric tracer for *β*-caryophyllene secondary organic aerosol. *Geophys. Res. Lett.* **2007**, *34*, No. L05816.
(103) Sharma, G.; Sinha, B.; Pallavi, P.; Hakkim, H.; Chandra, B. P.; Kumar, A.; Sinha, V. Gridded Emissions of CO, NO_x, SO_2, CO_2, NH_3, HCl, CH_4, $PM_{2.5}$, PM_{10} BC, and NMVOC from Open Municipal Waste Burning in India. *Environ. Sci. Technol.* **2019**, *53*, 4765−4774.
(104) Saikawa, E.; Wu, Q.; Zhong, M.; Avramov, A.; Ram, K.; Stone, E. A.; Stockwell, C. E.; Jayarathne, T.; Panday, A. K.; Yokelson, R. J. Garbage Burning in South Asia: How Important Is It to Regional Air Quality? *Environ. Sci. Technol.* **2020**, *54*, 9928−9938.
(105) Pallavi, P.; Sinha, B. Source apportionment of volatile organic compounds in the northwest Indo-Gangetic Plain using a positive matrix factorization model. *Atmos. Chem. Phys.* **2019**, *19*, 15467−15482.
(106) Chandra, B. P.; Sinha, V. Contribution of post-harvest agricultural paddy residue fires in the NW Indo-Gangetic Plain to ambient carcinogenic benzenoids, toxic isocyanic acid and carbon monoxide. *Environ. Int.* **2016**, *88*, 187−197.
(107) Islam, M. R.; Li, T.; Mahata, K.; Khanal, N.; Werden, B.; Praveen, P. S.; Dhital, N. B.; Gurung, A.; Panday, A. K.; Yokelson, R. J.; DeCarlo, P. F.; Stone, E. A., Field Campaign Data from NAMaSTE-2 at Lumbini in December 2017 - January 2018: $PM_{2.5}$ and PM_{10} mass, $PM_{2.5}$ chemical composition, and chemical mass balance model results. 2020.